# Dissociative recombination and dissociative excitation of $^4HeH^+$: Absolute cross sections and mechanisms

C. Strömholm,[1] J. Semaniak,[1] S. Rosén,[1] H. Danared,[2] S. Datz,[3] W. van der Zande,[4] and M. Larsson[1]
[1]*Department of Physics I, Royal Institute of Technology (KTH), S-100 44 Stockholm, Sweden*
[2]*Manne Siegbahn Laboratory, Stockholm University, S-104 05 Stockholm, Sweden*
[3]*Physics Division, Oak Ridge National Laboratory, Oak Ridge, Tennessee 37831-6377*
[4]*FOM-Institute for Atomic and Molecular Physics, Kruislaan 407, 1098 SJ Amsterdam, The Netherlands*
(Received 1 April 1996)

Absolute cross sections have been determined for the dissociative recombination and dissociative excitation of $^4HeH^+$ for electron energies below 40 eV. The dissociative recombination cross section is in semiquantitative agreement with recent theoretical results by Sarpal, Tennyson, and Morgan [J. Phys. B **27**, 5943 (1994)] and Guberman [Phys. Rev. A **49**, R4277 (1994); in *XIXth International Conference on the Physics of Electronic and Atomic Collisions, Whistler, Canada*, AIP Conf. Proc. No. 360, edited by L. J. Dube, J. B. A. Mitchell, J. W. McConkey, and C. E. Brion (AIP, New York, 1995), p. 307]. The calculated resonant structure below a collision energy of 1 eV was not fully reproduced by the experiment. The quantum states of the dissociative recombination products at 0 eV collision energy have been determined; ground-state helium and excited hydrogen atoms ($n=2$) are dominantly formed, in agreement with recent predictions by Guberman. The dissociative excitation has an onset around 10 eV and follows the shape of the dissociative recombination cross section, illustrating that both processes start with the formation of doubly excited neutral states that lie in the ionization continuum as well as in the dissociation continuum. The dissociative excitation cross section is in quite good agreement with recent calculations by Orel and Kulander. [S1050-2947(96)09310-9]

PACS number(s): 34.80.Gs, 34.80.Ht, 34.80.Kw, 34.80.Lx

## I. INTRODUCTION

Dissociative recombination is a process of quantitative importance in the chemistry of interstellar plasmas as it is the main destruction mechanism for molecular ions present in such environments. The difficulty to observe helium hydride (ions) in the interstellar medium [1] seemed in contradiction with predictions that $HeH^+$ could be abundant [2]. These predictions did not include the possibility of destruction of $HeH^+$ by dissociative recombination (DR). As was generally accepted at that time, the lack of a neutral repulsive potential-curve crossing the ground state of the molecular ion would prevent DR from taking place. Experiments by means of the Flowing Afterglow/Langmuir Probe technique [3] supported the view that recombination of $HeH^+$ is extremely slow. However, a simultaneous single-pass merged-beams experiment [4] showed a large dissociative recombination cross section difficult to reconcile with the theories at that time [5]. Later, heavy ion storage ring experiments [6,7] on $^3HeH^+$ carried out at CRYRING [8,9], and on $^4HeH^+$ and $^4HeD^+$ carried out at TARN II [10,11] confirmed the high dissociative recombination cross section at low collision energies. These observations encouraged a search for other mechanisms to explain a high cross section for DR without curve crossing.

Two different theories have shown a reasonable agreement with experimental results [12–14]. The magnitudes of the observed cross sections were reproduced. The interaction operator responsible for the DR process was found to be the nuclear kinetic-energy operator, which mixed the ionic continuum with the dissociation continuum around the inner turning point of the molecular ground state potential curve. The two theories displayed a different resonant structure for $^4HeH^+$ [12,14]. The theories also differed in their predictions of the states of the dissociation products. The *ab initio* calculations by Sarpal, Tennyson, and Morgan [12] predict both the helium and the hydrogen to be in their ground states, whereas Guberman's calculations for the isotopomers $^3HeH^+$ [13] and $^4HeH^+$ [14] predict the hydrogen to be in its $n=2$ state after dissociation. The TARN II experiment [11] included an estimate of the kinetic energy released upon dissociative recombination with a simple position sensitive detector. This experiment rendered support to the prediction by Guberman of a small kinetic energy release ($\sim$1 eV).

Electron capture in an electron-molecular ion collision does not necessarily lead to dissociative recombination. Electrons with sufficient energy may excite the molecule directly to a repulsive ionic state resulting in the dissociation of the molecular ion. An alternative pathway may go via the formation of a doubly excited neutral state that may autoionize to the vibrational continuum of the ground state ion, which also leads to dissociation. The latter dissociative excitation mode is in a direct competition with dissociative recombination. Both processes are called dissociative excitation (DE).

The present work was performed to test existing theories and to provide accurate data for astrophysical applications. We present high resolution absolute cross-section measurements of dissociative recombination of $^4HeH^+$ at electron collision energies below 40 eV. Data were taken in very small energy steps below 1 eV. The results are compared with theoretical predictions and the isotope effect is evaluated using earlier CRYRING results on $^3HeH^+$. Using a two-dimensional imaging detector, the final states of the DR fragments are determined at 0 eV collision energy. For practical,

 

interstellar chemistry, purposes the DR rates are evaluated at various electron temperatures. Dissociative excitation cross sections were determined from which the competition between DR and DE becomes apparent. DE is observed to start around 10 eV. A series of tests has been performed to check for systematic errors that may occur in heavy ion storage ring experiments.

## II. EXPERIMENT

The experiments were performed at the heavy ion storage ring CRYRING at the Manne Siegbahn Laboratory at Stockholm University. $^4HeH^+$ ions were created by mixing helium and hydrogen in a low-pressure plasma ion source. After mass selection, the ions were injected into the storage ring at an energy of 40 keV and further accelerated to an energy of 3.84 MeV/amu. The approximate number of injected ions was $9\times10^6$, as measured with a current transformer. The lifetime of the stored ions is dominated by collisions in the rest gas. The ambient pressure of $10^{-11}$ Torr resulted in a beam lifetime of approximately 15 seconds.

Two cooling mechanisms are operative in this experiment. First, the storage of the ions allows full vibrational relaxation through infrared emission resulting in a $HeH^+$ beam in the ground vibrational state. Second, the circulating ions are phase-space cooled by interacting with a collinear beam of velocity matched electrons in the electron-cooler section of the ring. The phase-space cooling allows for the ultimate energy resolution of the experiment. Acceleration of the electrons results in a longitudinal energy spread of about $kT_e=0.1$ meV. The temperature of the electron-cooler cathode (1000 K) results in a transverse temperature of $kT_e=0.1$ eV, which is reduced by a factor of 10 prior to the interaction region by using adiabatic expansion of the electron beam in a decreasing magnetic field [15]. The resolution in electron-collision energy is dependent on the magnitude of the center-of-mass energy. At energies lower than 1 eV it is given by the transverse energy spread of 10 meV.

The electron beam from the cooler also serves as a target in the dissociative recombination experiment. During the data taking, the electrons are alternatively detuned from the cooling energy $E_{\rm cool}$ to a new energy $E_{\rm meas}$ which is the laboratory energy of the electrons when a measurement is performed. The difference between the longitudinal velocities of the electron and ion beams when a measurement is performed is called the detuning velocity, $v_d$, which is associated with an energy, $E_d$, according to the relation $E_d=m_e v_d^2/2$. The detuning energy is related to the laboratory electron energies $E_{\rm cool}$ and $E_{\rm meas}$ through $\sqrt{E_d}=\sqrt{E_{\rm meas}}-\sqrt{E_{\rm cool}}$. When $E_d$ is larger than $kT_e$, the center-of-mass collision energy approaches the detuning energy [6,7].

The dissociative recombination measurements are performed within short temporal gates simultaneously created with the electron-cooler jumps. The latter jumps are made short enough to avoid drag-force effects, i.e., reduction of the detuning energy due to Coulomb interaction between electrons and ions.

The neutral dissociation products formed in the cooler section by rest-gas collisions, dissociative recombination, and dissociative excitation, proceed in a straight line through the bending magnet following the cooler section. The fragments are detected in the so called zero-degree beam line by an ion-implanted surface barrier detector (SBD) located approximately 4 meters from the center of the electron cooler. The spectra are recorded using a multichannel analyzer (MCA). A typical pulse-height spectrum, shown in Fig. 1, consists of three peaks; two corresponding to single hydrogen (at 3.84 MeV) and helium (at 15.36 MeV) atoms arising from collisions with rest-gas particles and, at high center-of-mass energies, dissociative excitation. The highest energy peak (at 19.2 MeV) implies that a helium and a hydrogen atom arrived simultaneously, which is representative for DR.

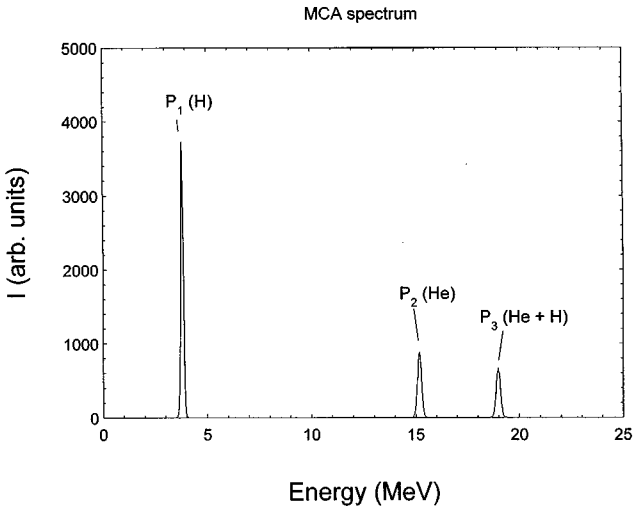


FIG. 1. A typical MCA spectrum used for the determination of the rate coefficient for dissociative recombination in the electron cooler. The figure shows the number of counts detected by the surface barrier detector as a function of the particle energy. The high energy peak is due to DR whereas the two other peaks result from collisions in the rest gas.

A multichannel scaler (MCS) was used to monitor the background signal from single hydrogen and helium as a function of time after injection of the ions. The number of injected ions was established with a current transformer. The MCS data and the ion current measurement were used to calculate the absolute destruction probability of the ions due to collisions with the rest gas. As will be explained below, this probability facilitates an absolute DR cross-section determination. At high electron collision energies, an increase in the background count rate coinciding with the electron cooler jumps is observed with the MCS. This increase is due to dissociative excitation. The background in an MCA spectrum is corrected for this DE process.

In order to check for possible systematic errors present in an ion storage ring experiment, experiments were performed at various electron currents (check for three-body collisions or field effects) and at various times after ion injection (check for time-dependent cross sections, and changes in the $HeH^+$ beam population in time).

In the present experiment we also used a two-dimensional imaging detector to measure the kinetic energy release in the dissociative recombination of $^4HeH^+$ molecules with electrons at detuning energy of 0 eV (i.e., $E_{\rm meas}=E_{\rm cool}$). This detection system has been described in [16] and is briefly described here.

The detector was installed in the zero-degree beam line at a distance of 5.9 m from the midpoint of the electron cooler. It consisted of three micro channel plates (MCP) stacked with a diameter of 18 mm. The impact of an energetic atom created a sharp and intense bunch of electrons (of the order of $10^7$), which were further accelerated towards a phosphorus screen placed at a distance of 7 mm from the last MCP. The electron pulse was transformed into a scintillation on the phosphorus screen and then imaged by a CCD camera and read out digitally. This system detected both the DR fragments as well as single neutral fragments produced by collisions with the rest gas. Therefore, the detector was operated in a trigger mode to reduce the background caused by random coincidences resulting from two uncorrelated single atoms. The trigger pulse used to switch off the MCP's was taken from the output of a fast photomultiplier tube monitoring the flashes on the phosphorus screen. Every flash (both due to single, rest-gas collision products and two-particle DR fragments) resulted in the switching off the MCP's in 40 s for a time of about 700 s. The integration time for one frame was about 900 s. This timing regime allowed the detection two DR fragments, which arrived in a time interval less than 1 ns, while it at the same time facilitated a significant suppression of random coincidences. The data were taken in the free running mode of the CCD camera at a rate of 1100 frames per second. The data were further processed so that the two-particle-event frames were identified and the distance between fragments calculated. The resolution of the detector was approximately 0.25 mm.

### III. DATA ANALYSIS

The absolute cross section can be determined by measuring the absolute destruction rate of the molecular ions by rest gas collisions and comparing the intensity of background and signal in one MCA spectrum. A typical MCA spectrum recorded at $E_d=0$ eV is shown in Fig. 1. Dissociative recombination of $^4HeH^+$ results in the formation of two neutral atoms according to the reaction:

$$^4HeH^+ + e + \text{collision energy} \rightarrow He + H(n) + \text{kinetic energy}. \quad (1)$$

Note that no signal is observed at 19.2 MeV without the cooler electrons. Thus all counts at this energy are caused by DR. The other peaks at 15.36 and 3.84 MeV correspond to fragments from rest-gas collisions. These signals should be independent of the electron cooler electrons and can be used for the normalization of the DR-count rate. The count rate due to DR ($Q_{DR}$) recorded by the detector is related to the absolute DR rate coefficient ($R_{DR}$ in $cm^3$ s) according to the following relation:

$$Q_{DR}=R_{DR}n_eN\left(\frac{l}{C}\right), \quad (2)$$

where $n_e$ is the electron density, $N$ is the number of stored ions, and $l/C$ is the ratio between cooler length and storage ring circumference ($l=0.85$ m, $C=51.6$ m) accounting for the fact that DR events take place only in the cooler section. Let $P_3$ be the integrated number of counts due to DR and $P_1$ the integrated number of counts of hydrogen atoms coming from background collisions registered in the MCA spectra. Then

$$P_3=R_{DR}n_e\left(\frac{l}{C}\right)\int_{\text{gates}}N(t)dt, \quad (3)$$

$$P_1=R_B\int_{\text{gates}}N(t)dt. \quad (4)$$

The time integration is made over the measuring gates. $R_B$ is the rest-gas destruction rate per ion and unit time in the cooler section of the ring. Dividing (3) with (4) gives the simple relation

$$R_{DR}=R_B\left(\frac{C}{n_el}\right)\frac{P_3}{P_1}. \quad (5)$$

The absolute destruction rate $R_B$ can be computed by relating the result of an ion current transformer measurement to the MCS measurement of the count rate of a hydrogen background peak. The ion current is a function of time and can be given as

$$I(t)=N(t)\frac{v_i}{C}q, \quad (6)$$

$v_i$ and $q$ being the ion velocity and ion charge, respectively. The background count rate recorded by the MCS is given by

$$\frac{dP_1}{dt}=R_bN(t). \quad (7)$$

By dividing (6) and (7), $N(t)$ disappears and $R_B$ can be computed by giving the MCS count rate and the ion current at a given time $t$. Subsequently, the reaction rate coefficient in the electron cooler for reaction (1) can be computed using Eq. (5).

At high electron collision energies (above 10 eV) the MCS spectra of the background were modulated synchronously with the electron cooler jumps. This background increase is corrected for in the computation of the DR rate. The magnitude of these changes directly gave a measure of the dissociative excitation cross section.

The above equations yield the DR rate coefficient *in the electron cooler* as a function of the detuning energy. These numbers can be converted to DR cross sections by employing a deconvolution procedure using the electron velocity distribution at detuning energies below 1 eV. At higher energies, where the electron-energy spread is negligible with respect to the collision energy, the cross section is obtained by dividing the rate coefficient, $R_{DR}$, with the electron velocity in the center-of-mass frame.

The measurement of the absolute current using the current transformer has an estimated error of 10%. This exceeds the statistical uncertainty involved in the measurements at low energies. At the entrance and exit from the cooler the electrons are not collinear with the ion beam. The magnetic field causes the electrons to have a radius of curvature of 0.4 m. At the ends of the electron cooler, the collision energy is increased, so that one also samples the DR cross section at

higher collision energy. The increment in collision energy may be as large as 250 eV for a nominal c.m. energy of 10 eV at our experimental conditions (i.e., with the beam energy we used). We estimated this effect by performing the calculations described in the work by Lampert *et al.* [17] to the first order. The observed rates are mostly affected close to the minimum at 1 eV by this toroidal magnetic field effect, where the large cross section of the high energy peak between 10 and 20 eV gives a contribution. However, this contribution is not very large since it represents only 4% of the merging region (1% of the total interaction region). The rest of the merging region contributes very little since one sample the very low cross section present at higher energies. The rate coefficient presented here is thus overestimated by at most 10% in the region between 1 and 10 eV, a correction which is barely visible in Fig. 3.

To examine if the rates were time dependent, for instance as a consequence of a slow vibrational relaxation in the $^4HeH^+$ ion beam, the DR rate was recorded at four different times after injection (3, 5, 10 and 15 s). No time dependence of the rate was observed in agreement with the predicted radiative relaxation times of at most 120 ms [18].

Finally a series of experiments was performed at four different electron currents (9, 25, 54, and 100 mA). An increased electron density could possibly give rise to three-body effects. This would perturb the measurement since we are only interested in one electron–one ion reactions. The test was performed at a detuning energy of 0.22 eV. Formula (5) suggests that the DR signal divided by the signal coming from background gas collisions ($P_3/P_1$) is proportional to the electron density in the absence of three-body effects. The measured ($P_3/P_1$) also showed a linear dependence on the electron current from which it was concluded that three-body effects are not important under our circumstances. The same test was also performed with a detuning energy of 0 eV. It was found that the apparent cross-section was higher for lower currents contradictory to formula (5). It has, however, been shown in a work by Schuch [19] that the energy resolution (electron temperature) is depending on the electron density implying that the resolution deteriorates for higher electron currents. This affects the results for very low detuning energies ($E_d \leqslant kT_{e\perp}=0.01$ eV). That is why we chose to perform the three-body effect test for a higher detuning energy (i.e., $E_d=0.22$ eV).

The two-dimensional imaging detector measured the transverse separation of the DR fragments at a distance $L$ from the electron cooler. The transverse separation is determined by the kinetic energy release (KER) in the center-of-mass frame and can be expressed by the following formula:

$$D=\sqrt{\frac{E_{\mathrm{KER}}}{E_u\mu}}\,L\,\sin\theta \tag{8}$$

where $E_u$ is the beam energy (in MeV/amu), $\mu$ is the reduced mass of the molecular ion, and $\theta$ is the angle of the molecular axis during dissociation with respect to the electron beam. The KER is determined by the initial and final quantum energy states of the participating particles (the parent molecular ion and two atomic products) and the collision energy.

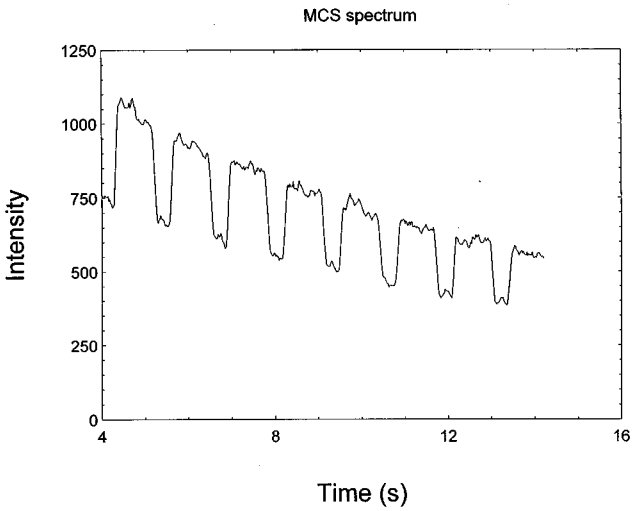


FIG. 2. An MCS spectrum following the time evolution of the signal from single hydrogen atom during one injection and including 10 electron cooler jumps. The decay of the beam and the increase in the signal due to DE are clearly observed. The time axis is in seconds after injection.

For the given KER and isotropic fragmentation of molecular ions the measured spectrum of transverse separations can be described by an analytical function [20] as follows:

$$P(D)=\frac{1}{D_{l+L}-D_l}\left\{\arccos\left[\min\left(1,\frac{D}{D_{l+L}}\right)\right]-\arccos\left[\min\left(1,\frac{D}{D_l}\right)\right]\right\}, \tag{9}$$

where $l$ is the effective length of the electron-ion interaction region and $D_L$ and $D_{l+L}$ correspond to the maximum projected distance between DR fragments created at the entrance and at the exit of the electron cooler section.

The last part of the experimental results deals with the experimental determination of the dissociative excitation cross-sections and their comparison with the DR results. Dissociative excitation is a process where an electron collisionally excites a molecular ion to a dissociative state or to a short lived predissociating state. In the case of $^4HeH^+$ two channels can be distinguished with different energetic thresholds:

$$^4HeH^+ + e \rightarrow {}^4HeH^{+}* \rightarrow H^+ + {}^4He \tag{10a}$$

or

$$\rightarrow H + {}^4He^+. \tag{10b}$$

Since the reactions lead to only one neutral atom, they are not as easily detected as the DR reaction. The neutral hydrogen or helium atoms from DE are severely blended by those coming from rest-gas collisions. A typical MCS spectrum of hydrogen, where the electron cooler is detuned to give a c.m. energy of 34 eV, is shown in Fig. 2. The DE rate ($Q_{\mathrm{DE}}$) is calculated as the count rate during the cooler jumps ($Q_{\mathrm{CJ}}$) decreased by the count rate between the cooler jumps ($Q_B$). The relation between the experimental rate and the rate co-

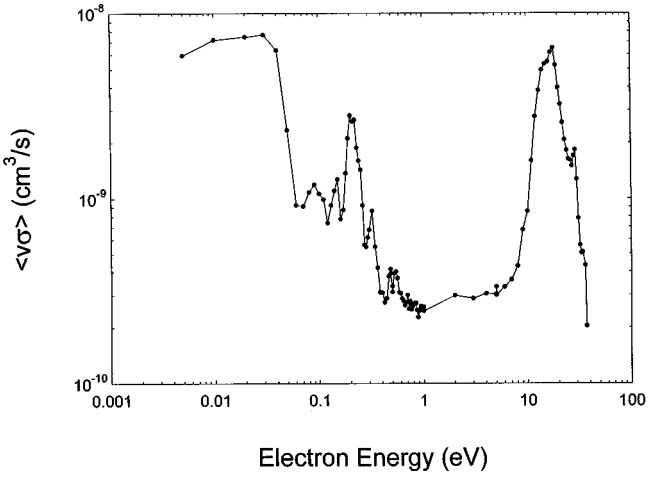


FIG. 3. Rate coefficient as a function of the detuning energy for dissociative recombination of $^4HeH^+$.

efficient of the DE reaction is found in a way very similar to the method used to extract the rate coefficient for DR. Equation (5) can be utilized the same way as previously with some minor changes. The DE rate coefficient is thus found from

$$R_{\mathrm{DE}}=R_B\,\frac{C}{n_e l}\,\frac{(Q_{\mathrm{CJ}}-Q_B)}{Q_B}. \tag{11}$$

Reactions (10a) and (10b) were studied separately by recording MCS spectra at various electron energies for helium atoms and for hydrogen atoms, respectively. The DE rate was measured for electron energies ranging from 1 to 37 eV with a step of 1 eV. The absolute cross section was simply extracted by dividing the rate coefficient with the electron velocity in the center-of-mass frame $\sigma_{\mathrm{DE}}=R_{\mathrm{DE}}/v_{\mathrm{rel}}$.

## IV. RESULTS AND DISCUSSION

### A. Dissociative recombination

Using the procedures given in the previous section, the DR rate coefficient in the electron cooler was measured at various center-of-mass energies ranging from 0.005 to 35 eV. The result is shown in Fig. 3. The step size was chosen to be small at energies up to 1 eV in order to resolve narrow resonances in this region due to indirect DR mechanisms in which molecular Rydberg states play a role. The energy resolution is 10 meV below 1 eV. Indeed, at low electron energies, structures can be observed. The general trend is a DR rate which decreases with energy. At higher electron energy a broad maximum is observed starting near 10 eV.

Figure 4 contains a summary of the electronic states that are important for the results. The $X\ ^1\Sigma^+$, $A\ ^1\Sigma^+$, and $a\ ^3\Sigma^+$ states in $HeH^+$ are shown. The neutral ground state is repulsive which is indicative for the unstable nature of HeH. The $C\ ^2\Sigma^+$ Rydberg state is shown; it is a candidate for the primary dissociation route in low-energy DR. In the ionization continuum a number of doubly excited neutral states are indicated that are important for the high-energy features in the DR spectra and for all features in the DE process.

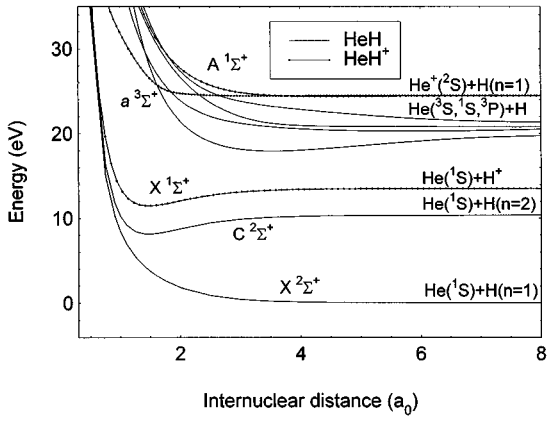


FIG. 4. Potential curves for $^4HeH^+$ and $^4HeH$ relevant for this work. These are found in, e.g., Refs. [4] and [12].

The discussion is divided in a low-energy region from zero to approximately 1 eV and the high-energy region from 1 to 40 eV. A cross section for the high-energy region can be extracted simply by dividing $R_{\mathrm{DR}}$ with the electron velocity in the center-of-mass frame. We will start to describe this region. The high-energy region contains one broad asymmetric feature with a maximum at 18 eV, as shown in Fig. 5. It very much resembles the high energy structure of $^3HeH^+$ in a previous experiment both in terms of absolute cross section as well as in position [8]. The irregular shape clearly indicates that it is composed of contributions from several resonances. A shoulder is present at 14 eV and a small peak at 28 eV. A recent theoretical study by Orel, Kulander, and Rescigno [21] treats the dissociative recombination of $^3HeH^+$ in this energy region. The process is explained by an intermediate capture of an electron into a Rydberg orbital of HeH. The ionic core of this neutral doubly excited molecule is called the parent ion. Two parent ionic states are considered here, namely $a\ ^3\Sigma^+$ and $A\ ^1\Sigma^+$. These states are steeply repulsive in the Franck-Condon region, so that the probability for dissociation becomes larger than that for autoionization.

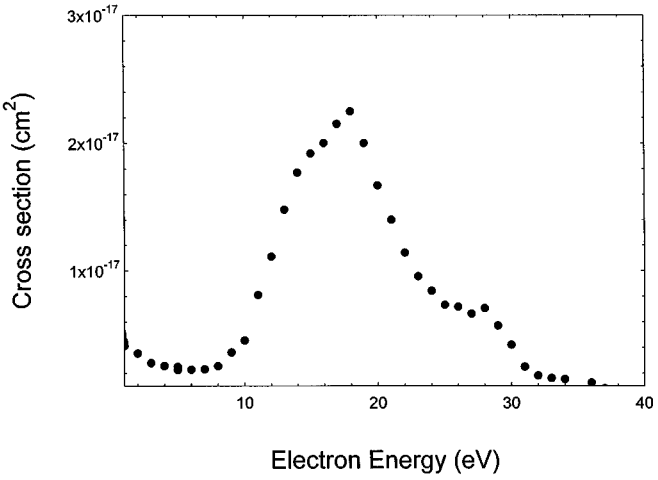


FIG. 5. DR of $^4HeH^+$ for energies ranging from 1 to 40 eV. The broad structure centered at 18 eV is mostly due to capture into a doubly excited Rydberg state, which subsequently dissociate.

These resonances have an important capture probability and play a dominant role for the DR cross section. The calculation by Orel, Kulander, and Rescigno [21] included eight doubly excited neutral states, four $^2\Sigma$ states and one $^2\Pi$ state with the $a\ ^3\Sigma^+$ state as a parent ion state, and the two lowest neutral states associated with the $A\ ^1\Sigma^+$ state. The $(1\sigma 3\sigma^2)$ state dissociating to He($2\ ^3S$) plus excited hydrogen is also included. The results agree quite well both in shape and magnitude with the experimental $^3HeH^+$ cross section. Only the shoulder near 30 eV is not found in the calculations. The absence of a strong isotope effect corroborates the electronic nature of the resonances involved.

For low collision energies the non-negligible velocity spread of the cooler electrons has to be taken into account. The relation between the rate coefficient and the cross section is given by

$$R_{\mathrm{DR}}=\langle v\,\sigma\rangle=\int_0^\infty f(v_d,\mathbf{v})\sigma(v)v\,d^3v, \tag{12}$$

where $\mathbf{v}$ is the vector of relative velocity between an electron and an ion and $v$ is its magnitude. The function $f(v_d,\mathbf{v})$ is the relative velocity distribution. The electron velocity distribution is expressed as a product between two Maxwell-Boltzmann distributions to account for the different distributions parallel and perpendicular to the ion beam direction. The relative velocity distribution is thus described by two temperatures [22]

$$f(v_d,\mathbf{v})=\frac{m}{2\pi kT_\perp}\exp\left(\frac{-mv_\perp^2}{2kT_\perp}\right)\times\left(\frac{m}{2\pi kT_\parallel}\right)^{1/2}\exp\left(\frac{-m(v_\parallel-v_d)^2}{2kT_\parallel}\right) \tag{13}$$

and denotes movement perpendicular and parallel to the ion beam, respectively. Relation (13) can be considerably simplified by realizing that $T_\parallel \ll T_\perp$. Setting $T_\parallel=0$ yields the following for $f(v_d,\mathbf{v})$:

$$f(v_d,\mathbf{v})=\frac{m}{2\pi kT_\perp}2\pi v\ \exp\left(-m\,\frac{v^2-v_d^2}{2kT_\perp}\right)H(v-v_d),$$

$$H(v-v_d)=1,(v-v_d)>0,$$

$$H(v-v_d)=0,(v-v_d)<0. \tag{14}$$

Introduction of the collision energy $E=mv^2/2$ gives the following expression for the rate coefficient as a function of the detuning energy:

$$R_{\mathrm{DR}}(E_d)=\frac{1}{kT}\int_0^\infty \sigma(E+E_d)\exp\left(-\frac{E}{kT}\right)dE. \tag{15}$$

The integral represents the convolution between the cross section and an instrumental function coming from the electron-velocity distribution. The cross section can be found by using the technique of Fourier transforms. Fourier transforming both sides of Eq. (15) gives

$$\mathcal{F}(R_{\mathrm{DR}})=\mathcal{F}(\sigma)\mathcal{F}(f\ ). \tag{16}$$

$f=f(v_d,\mathbf{v})$ is the instrumental function determined by the electron-velocity distribution. The cross section is then found by applying an inverse Fourier transform, according to

$$\sigma(v)=\frac{1}{v}\,\mathcal{F}^{-1}\left\{\frac{\mathcal{F}(R_{\mathrm{DR}})}{\mathcal{F}(f\ )}\right\}. \tag{17}$$

This method has been employed to extract the cross section from the rate coefficient using a numerical fast Fourier transform algorithm of MATLAB [23]. The computed cross section was subsequently used for the determination of the thermal rate coefficient described in the last part of this section. The general decrease of the cross section with increasing energy is related to the Wigner threshold law ($\sigma\propto E^{-1}$). In cross-section calculations many much sharper resonances are found and attributed to the location of certain vibrational excited states in HeH Rydberg states. DR via these Rydberg states is called indirect DR, since the neutral, vibrationally excited Rydberg state is subsequently predissociated. The magnitude of the experimental cross section ($10^{-15}$ cm$^2$ at 0.02 eV) is considerable despite the lack of potential curve crossing. In the case of $H_2^+$ ($v=1$), cross sections are reported of $1\times10^{-14}$ cm$^2$ at 0.02 eV [24]; this is considered the classic case of a curve crossing. It is again concluded that the DR of $^4HeH^+$ and its isotopomers [8–11] is an efficient process at low electron energies. The mechanism of the dissociative recombination process in this region is no longer a question of debate. The coupling between the ionization continuum and the neutral dissociative states is due to the nuclear kinetic-energy operator. The low energy DR is explained in terms of tunneling from the inner turning point of the $^4HeH^+$ potential curve to states of the neutral molecule situated at smaller internuclear distance (see Fig. 4). Two recent theoretical reports exist on this mechanism using different computational techniques. Guberman [13,14] employed a multichannel quantum-defect theory (MQDT) approach, whereas Sarpal, Tennyson, and Morgan [12] made use of $R$-matrix theory. The tunneling mechanism is expected to be strongly isotope dependent. In a direct way because of the occurrence of the reduced mass in the kinetic energy operator and more indirectly because of the overlap in the classically forbidden region near the inner turning point of the ground-state potential curve.

Figure 6 contains a comparison of the measured rate coefficient with an earlier experimental study of $^3HeH^+$ at CRYRING [9]. Figure 7 compares our present results with the theoretical predictions of Sarpal, Tennyson, and Morgan [12] and Guberman [14]. In order to compare our results with the *ab initio* calculations, we performed a numerical convolution of the calculated cross sections with an instrumental function defined by the thermal spread of the electrons. The cross section of the light isotope is found to be larger by about 20–25 %, in agreement with the dependence of the kinetic operator on the inverse of the reduced mass. The $^3HeH^+$ [9] and the $^4HeH^+$ results show striking similarities even in the resonance structure: the steep falloff at 50 meV, the first broad structure around 100 meV, and the resonance near 200 meV are reproduced. The resonances in $^4HeH^+$ are shifted by 30 meV towards lower energy compared with $^3HeH^+$. The steep fall of the theoretical rate at 250 meV is due to the convolution procedure. The two theo-

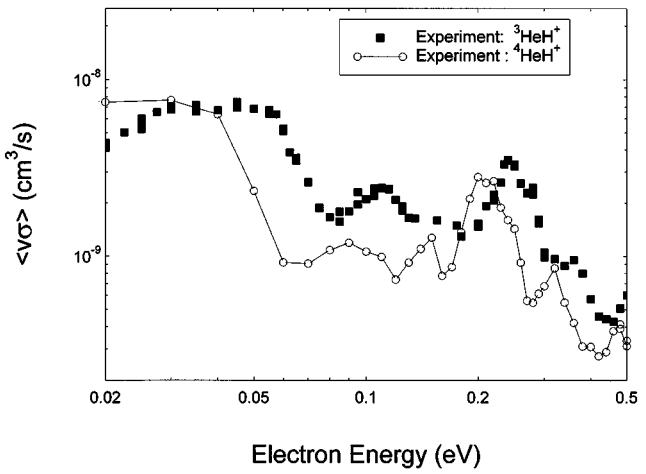


FIG. 6. Comparison of the experimental rate coefficient [$\langle v\sigma\rangle$ in Eq. (12)] for DR of $^4HeH^+$ and $^3HeH^+$. The latter is found in Ref. [9].

retical approaches [12–14] give rather different predictions. The theoretical calculations by Sarpal gives a better description of the fall off of the cross section below 100 meV. Apart from a 10 meV shift the resonances seem to be described somewhat better by the MQDT calculations by Guberman [14]. The magnitude of the rate is rather well described suggesting that indeed the role of the nuclear kinetic-energy operator can be important in driving DR of $HeH^+$.

A very practical quantity is the thermal rate coefficient: the reaction rate of DR in an environment in thermodynamical equilibrium. The thermal rate coefficient is computed by folding the cross section with a thermal electron-velocity distribution. We note that we cannot account for the adaptation of the $HeH^+$ ion population to the temperature; in particular the effect of the rotational excitation. The expression for the thermal rate coefficient, denoted by the symbol $\alpha(T)$, is given by the following expression:

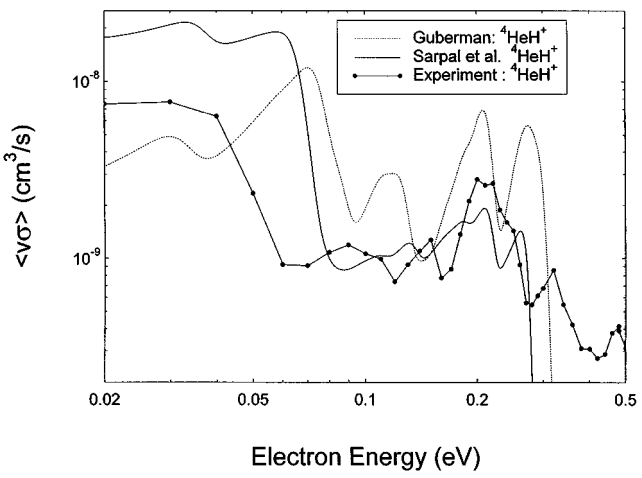


FIG. 7. Comparison of the experimental rate coefficient [$\langle v\sigma\rangle$ in Eq. (12)] for DR of $^4HeH^+$ and the theoretical calculations by Sarpal, Tennyson, and Morgan [12] and Guberman [14].

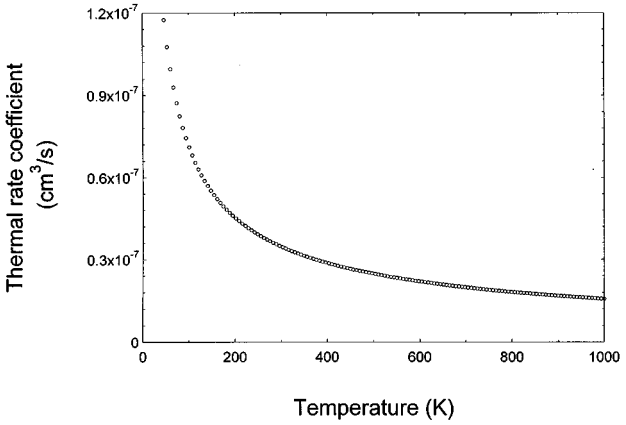


FIG. 8. Thermal rate coefficient for DR of $^4HeH^+$ for temperatures ranging from 20 to 1000 K.

$$\alpha(T)=\left(\frac{m}{2\pi kT}\right)^{(3/2)}\int_0^\infty v\,\sigma(v)\exp\left(-\frac{mv^2}{2kT}\right)4\pi v^2 dv. \tag{18}$$

The integration was performed numerically for temperatures ranging from 20 to 1000 K and the result is shown in Fig. 8. We note that the rate coefficient at 300 K is about $3\times10^{-8}$ cm$^{-3}$, which is three orders of magnitude higher than was anticipated in estimates of the $HeH^+$ abundance in the interstellar medium [2].

### B. Product state distributions

Figure 9 shows the transverse separation distribution measured at $E_{\text{c.m.}}=0$ eV. At this energy only two dissociation limits are energetically allowed for $^4HeH^+$ ions in their zeroth vibrational level of the electronic ground state ($X^1\Sigma^+$). One of them is when both fragments are in their ground states; the second one includes the excited H* fragment in the $n=2$ state. The kinetic energy releases corresponding to these limits are equal to 1.56 and 11.76 eV, respectively

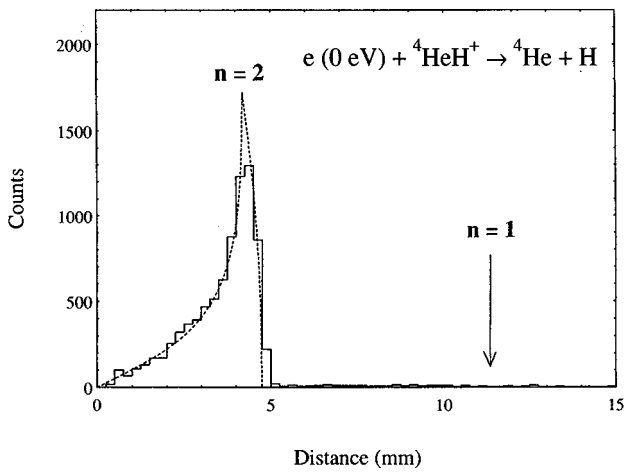


FIG. 9. Distribution of projected distances between the dissociation fragments measured at $E_d=0$ eV (solid line). The dashed line shows the theoretical distribution calculated according to formula (9) for the KER=1.49 eV.

(according to the $^4HeH^+$ ground state potential curve calculation by Wolniewicz [25], the H and He atomic states calculation by Miller and Schaefer [26], and data from Huberg and Herzberg [27] to calculate the zero-point energy).

The solid line in Fig. 9 shows the projected distance distribution calculated according to formula (9) for a kinetic energy release of KER=1.49 eV. It is in excellent agreement with the measured spectrum. The energetic uncertainty of this result corresponding to a distance resolution of 0.25 mm was estimated to be about 0.2 eV in that energy range.

The kinetic energy release for the dissociative recombination of $^4HeD^+$ ions at $E_{c.m.}=0$ eV has been measured only by the TARN II group [11]. They estimated the KER on the level of $1.0\pm0.5$ eV using a simple detection technique. Their estimation is in agreement with our result.

The present result indicates that at a collision energy close to 0 eV, the dissociation of $^4HeH^+$ ions results primarily in excited H*($n=2$) fragments [no distribution corresponding to the He+H($n=1$) limit]. The lack of any structure at larger distances excludes vibrational excitation in the stored ions. The spatial distribution of the DR fragments is isotropic.

The present result confirms an assumption that the DR, being a nonadiabatic process, leads to the channels nearest in energy. It is in agreement with Guberman's calculations [13,14] performed with the MQDT approach. These calculations show that the $C^2\Sigma^+$ state is the dominant dissociative channel resulting in excited H*($n=2$) fragments. At $E_{c.m.}=0.001$ eV the calculated cross sections for DR along the two lowest neutral states ($X^2\Sigma^+$ and $A^2\Sigma^+$) are three to four orders of magnitude smaller than for $C^2\Sigma^+$ state.

Our result is contrary to the calculations carried out by Sarpal, Tennyson, and Morgan [12] using the $R$-matrix method. This theory predicts an opposite tendency in the branching probabilities below $E_{c.m.}=0.06$ eV: the cross section to the $X^2\Sigma^+$ ground state is over an order of magnitude larger than to the higher lying $A^2\Sigma^+$ and $C^2\Sigma^+$ states. Contrary to Guberman's predictions, it has also been foreseen that between 0.06 and 0.8 eV DR through the $A^2\Sigma^+$ state dominate over DR through the $C^2\Sigma^+$ state. Since both states result in the same dissociation limit [He+H*($n=2$)], they cannot be distinguished experimentally.

The measured data confirm that high DR cross sections can be found in $^4HeH^+$ in the low energy range where there is no crossing of double excited, neutral potential curves with the ion curve. The explanation suggested by Yousif *et al.* [28] associates the relatively high DR cross section with the metastable $a\ ^3\Sigma^+$ state. Since the kinetic energy release in that case is close to 0.2 eV, one can exclude this suggestion on the basis of out KER data.

### C. Dissociative excitation

The cross sections for the two different dissociation channels (10a) and (10b) are presented in Fig. 10.

First we examine the process (10b). The cross section shows a steep rise at 16 eV, considerably above the energetic threshold, and reaches a plateau at around 24 eV. This coincides more or less with the vertical excitation energies from the ground state to the first excited ionic states $a\ ^3\Sigma^+$ and $A^1\Sigma^+$ (16.8 and 25 eV, respectively). Dissociative excitation has been studied before in a single-pass merged-beams experiment by Yousif and Mitchell [4] and by theoretical calculations [29]. The cross section was found to have sharp maxima at 20, 26, and 38 eV. We find the cross section to be more or less constant at a level of $2.6–2.8\times10^{-17}$ cm$^2$ between 21 and 37 eV.

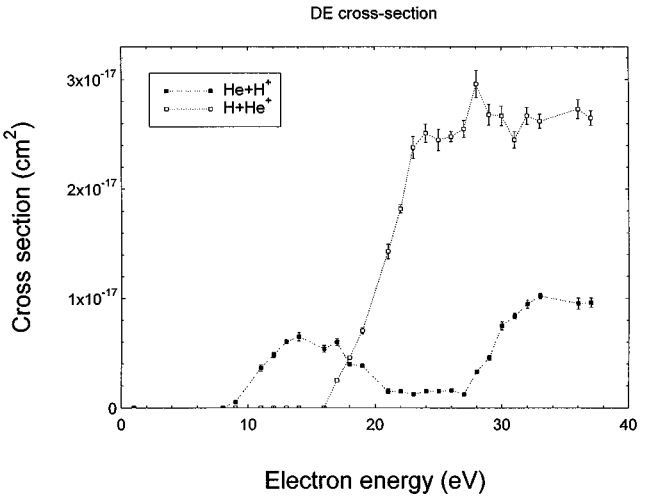


FIG. 10. Dissociative excitation of $^4HeH^+$ for collision energies ranging from 1 to 37 eV.

Of course, the energy region of interest also contains Rydberg series converging to these excited ion states. Electron capture into these states leads to the formation of doubly excited neutral HeH, which can undergo autoionization, dissociative autoionization, or dissociation [21]. Indeed, at these energies also the DR results show an appreciable cross section. The indirect mechanism, electron capture followed by dissociative autoionization, is very probably responsible for reaction (10a), i.e., the production of He+H$^+$ above 10 eV. We note that the energy required to reach an excited ion state dissociating to a neutral helium and a hydrogen ion in a vertical transition is about 30 eV coinciding with the second maximum in the He+H$^+$ channel. The dissociative excitation starts at 10 eV, very close to the rise of the high energy resonance in the DR reaction, which clearly points at a common origin. Dissociative excitation in that region competes with DR since there is a probability that the doubly excited neutral molecule can autoionize before dissociation. Calculations by Orel and Kulander [30] with the same neutral states as the ones used to reproduce the high energy DR peak [21] give excellent agreement with the experimental data with respect to the position and shape of the first maximum. The calculations overestimate the cross section by a factor of 2, compared with the experimental values.

## V. CONCLUSIONS

The noncurve crossing mechanism (denoted tunneling mode by Bates [31]) of dissociative recombination has been confirmed quantitatively by measuring absolute DR cross sections over a large collision-energy range for $^4HeH^+$. The observed resonance structure at low energy does not give a preference to any of the two existing theoretical predictions using an $R$-matrix method [12] and an MQDT method [13,14]. Product state information obtained at threshold supports the predictions by MQDT [13,14] that the formation of

excited state hydrogen ($n=2$) dominates dissociative recombination of $HeH^+$. We have simultaneously determined the absolute dissociative excitation cross section which shows a first resonance around 10 eV at the same place where structure can be found in the DR cross section; both processes start with the formation of doubly excited neutral states, which either autoionize in the dissociation continuum (DE) or dissociate (DR).


## ACKNOWLEDGMENTS

We would like to thank A. E. Orel, S. L. Guberman, and R. Schuch for communicating unpublished results. B. Sarpal is acknowledged for supplying cross-section results in a tabular form. W.v.d.Z. thanks the Foundation for Fundamental Research on Matter for financial support. The staff members of the Manne Siegbahn Laboratory are gratefully acknowledged for valuable help with the experiments.



[1] J. M. Moorhead, R. P. Lowe, J. P. Maillard, W. H. Wehlau, and P. F. Bernath, Astrophys. J. **326**, 899 (1988).

[2] W. Roberge and A. Dalgarno, Astrophys. J. **255**, 489 (1982).

[3] N. G. Adams and D. Smith, in *Dissociative Recombination: Theory, Experiment and Applications*, edited by J. B. A. Mitchell and S. L. Guberman (World Scientific, Singapore, 1989), p. 124.

[4] F. B. Yousif and J. B. A. Mitchell, Phys. Rev. A **40**, 4318 (1989).

[5] H. H. Michels, in *Dissociative Recombination: Theory, Experiment and Applications*, edited by J. B. A. Mitchell and S. L. Guberman (World Scientific, Singapore, 1989), p. 97.

[6] M. Larsson, Rep. Prog. Phys. **58**, 1267 (1995).

[7] M. Larsson, Int. J. Mass Spectrom. Ion Proc. **149/150**, 403 (1995).

[8] G. Sundström, S. Datz, J. R. Mowat, H. Danared, M. Carlson, L. Broström, S. Mannervik, and M. Larsson, Phys. Rev. A **50**, 2806 (1994).

[9] J. R. Mowat, H. Danared, G. Sundström, M. Carlson, L. H. Andersen, L. Vejby-Christensen, M. af Ugglas, and M. Larsson, Phys. Rev. Lett. **74**, 50 (1995).

[10] T. Tanabe, I. Katayama, N. Inoue, K. Chida, Y. Arakaki, T. Watanabe, M. Yoshizawa, S. Ohtani, and K. Noda, Phys. Rev. Lett. **70**, 422 (1993).

[11] T. Tanabe, I. Katayama, N. Inoue, K. Chida, Y. Arakaki, T. Watanabe, M. Yoshizawa, M. Saito, Y. Haruyama, K. Hosono, T. Honma, K. Noda, S. Ohtani, and H. Takagi, Phys. Rev. A **49**, R1531 (1994).

[12] B. K. Sarpal, J. Tennyson, and L. A. Morgan, J. Phys. B **27**, 5943 (1994).

[13] S. L. Guberman, Phys. Rev. A **49**, R4277 (1994).

[14] S. L. Guberman, in *XIXth International Conference on the Physics of Electronic and Atomic Collisions, Whistler, Canada*, AIP Conf. Proc. No. 360, edited by L. J. Dubé, J. B. A. Mitchell, J. W. McConkey, and C. E. Brion (AIP, New York, 1995), p. 307.

[15] H. Danared, G. Andler, L. Bagge, C. J. Herrlander, J. Hilke, J. Jeansson, A. Källberg, A. Nilsson, A. Paál, K.-G. Rensfelt, U. Rosengård, J. Starker, and M. af Ugglas, Phys. Rev. Lett. **72**, 3775 (1994).

[16] J. Semaniak, S. Rosén, G. Sundström, C. Strömholm, S. Datz, H. Danared, M. af Ugglas, M. Larsson, W. van der Zande, Z. Amitay, D. Zajfman, U. Hechtfisher, M. Grieser, R. Repnow, M. Schmidt, D. Schwalm, and A. Wolf, Phys. Rev. A (submitted).

[17] A. Lampert, A. Wolf, D. Habs, J. Kettner, G. Kilgus, D. Schwalm, M. S. Pindzola, and N. R. Badnell, Phys. Rev. A **53**, 1413 (1996).

[18] S. Datz and M. Larsson, Phys. Scr. **46**, 343 (1992).

[19] R. Schuch (private communication).

[20] D. Zajfman, Z. Amitay, C. Broude, P. Forck, B. Seidel, M. Grieser, D. Habs, D. Schwalm, and A. Wolf, Phys. Rev. Lett. **5**, 814 (1995).

[21] A. E. Orel, K. C. Kulander, and T. N. Rescigno, Phys. Rev. Lett. **74**, 4807 (1995).

[22] L. H. Andersen and J. Bolko, Phys. Rev. A **42**, 1184 (1990).

[23] MATLAB is a registered trademark of The Math Works, Inc.

[24] I. Schneider, O. Dulieu, and A. Giusti-Suzor, J. Phys. B **24**, L289 (1991).

[25] L. Wolniewicz, J. Chem. Phys. **43**, 1087 (1965).

[26] W. H. Miller and H. F. Schaefer III, J. Chem. Phys. **53**, 1421 (1970).

[27] K. P. Huber and G. Herzberg, *Molecular Spectra and Molecular Structure. IV. Constants of Diatomic Molecules* (VNR, New York, 1979), p. 300.

[28] F. B. Yousif, J. B. Mitchell, M. Rogelstad, A. Le Paddelec, A. Canosa, and M. I. Chibisov, Phys. Rev. A **49**, 4610 (1994).

[29] A. E. Orel, T. N. Rescigno, and B. H. Lengsfield III, Phys. Rev. A **44**, 4328 (1991).

[30] A. E. Orel and K. C. Kulander, Phys. Rev. A (to be published).

[31] D. R. Bates, Adv. At. Mol. Opt. Phys. **34**, 427 (1994).